Biophysical Chemistry, 39 (1991) 253–265

BIOCHE 01545

Time-resolved fluorescence emission and excitation spectroscopy of d(TA) and d(AT) using synchrotron radiation *

J.-P. Ballini [a], M. Daniels [b] and P. Vigny [a]

[a] *Laboratoire de Physique et Chimie Biomoléculaire (CNRS UA 198), Institut Curie et Université Paris VI, 11 rue Pierre et Marie Curie, 75231 Paris Cedex 05, France and* [b] *Chemistry Department and Radiation Center, Oregon State University, Corvallis, OR 97331-5903, U.S.A.*

Received 21 May 1990
Revised manuscript received 17 October 1990
Accepted 17 October 1990

Time-resolved excitation spectrum; Time-resolved emission spectrum; Stacked absorption; Stacked emission; Sequence isomer; Synchrotron radiation; Excited dimer

The photophysics of the sequence isomers d(TA) and d(AT) has been investigated at room temperature in 5×10^{-5} M neutral aqueous solution using pulsed ultraviolet excitation from the ACO synchrotron and detection by time correlation or gated single-photon counting. Decay profiles of the emissions at 350, 400 and 460 have been analyzed both independently and globally by reiterative non-linear least-squares fitting to models of two and three independently emitting species. No evidence has been observed for excited-state reaction. Time-windowed spectra, both emission and excitation, have been collected for three time windows and have been deconvoluted to give time-resolved spectra using the lifetimes resulting from the decay analyses. Spectra are separated into two classes, with picosecond and nanosecond lifetimes, respectively. The picosecond spectra have the emission and excitation spectral characteristics of mixed monomer (A and T) fluorescences and are assigned as originating from the unstacked fractions of d(TA) and d(AT). The nanosecond emission spectra from d(TA) and d(AT) are both two-component, with $\lambda_{max} \sim 350$ and ~ 425 nm and lifetimes of 2.3 and 6.1 ns, respectively. The time-resolved excitation spectra for the nanosecond emissions are quite different from the isotropic absorption spectra of d(TA) and d(AT) but correlate with the anisotropic absorption for out-of-plane transitions between stacked bases of co-crystals of 9-methyladenine and 1-methylthymine reported by Stewart and Davidson. The nanosecond spectra thus represent the direct excitation and emission of stacked pairs of bases. These results provide no evidence for energy transfer and are probably related to sequence-specific photo-adduct formation.

Correspondence address: J.-P. Ballini, Laboratoire de Physique et Chimie Biomoléculaire (CNRS UA 198), Institut Curie et Université Paris VI, 11 rue Pierre et Marie Curie, 75231 Paris Cedex 05, France.

Abbreviations: d(AT), deoxyadenylyl-3′,5′-deoxythymidylate (dApT); d(TA), deoxythymidylyl-3′,5′-deoxyadenylate (TpdA); DNPs, dinucleoside phosphates.

* Laboratoire d'Utilisation du Rayonnement Electromagnétique (LURE), CNRS and Université Paris-Sud, Bât. 209C, F-91405 Orsay Cedex, France. Presented at the Third Congress of European Society for Photobiology, Budapest, Hungary, 27 August-2 September, 1989.

1. Introduction

Some time ago, when investigating the temporal behavior of the weak room-temperature fluorescence from a natural DNA (calf thymus), we obtained evidence for a long-lived (nanosecond) emission [1]. As all the evidence available at that time [2] indicated that fluorescences from the individual nucleic acid base chromophores had lifetimes in the low (or sub-) picosecond range, this suggested to us that we were observing an ex-

cimer-type emission originating in the effects of the geometry of base stacking on the electronic states of the bases. The observation of a similar lifetime emission from poly d(AT) supported this assignment and opened the possibility that the DNA emission may be originating from (AT)/(TA) stacked pairs or from other AT sequences. These observations clearly indicated the need for further systematic studies on the effect of base stacking using simpler systems, and we now report a study of a prototype 'dimeric' system consisting of the sequence isomers d(AT) and d(TA).

In aqueous solution at ambient temperatures DNPs are well-known to exist in an equilibrium of stacked and unstacked conformers. On excitation of such a system the unstacked conformers will tend to exhibit spectral characteristics of their constituent 'monomer' chromophores (which do not live long enough to form excimer states by conformational re-ordering) while the stacked conformers may already be in a spatial orientation conducive to formation of an excimer-like state, recognized by their emissions which are red-shifted from the monomers and have nanosecond lifetimes [2]. The total emission spectrum observed on continuous excitation thus consists of overlapping monomer and excimer-like components which cannot be resolved without the input of other independently determined parameters. Two approaches are currently being exploited. The first utilizes the fact that monomer emissions are strongly polarized at room temperature [3a,b] while excimer-like emissions are rotationally depolarized [4a,b], leading to the technique of polarization-resolved spectroscopy. Resolutions on this basis have been reported for CpC [4a], CpA [5a] and ApC [5b]. The second approach directly utilizes the lifetime differences of the monomer and excimer-like components in the more familiar technique of time-resolved spectroscopy, based on the use of pulsed excitation together with time-gated detection. Given monomer lifetimes in the range of less than 6 ps and excimer-like lifetimes from 1 to 10 ns, an ideal excitation source for completely instrumental resolution of spectra should have a clean pulse-width of approx. 100 fs (together with a detector of picosecond resolution). The source available to us, the ACO-based synchrotron at LURE, Orsay, France, has a pulse-width of approx. 1.7 ns and this has two consequences for the present work. First, the extraction of low nanosecond lifetimes from decay data and of time-resolved spectra from time-windowed spectra requires extensive post-acquisition deconvolution of data. Second, true monomer lifetimes are beyond the resolution of the apparatus, which has a channel width of 78 ps; numbers for the fast (picosecond) lifetimes which are given by the data analysis (see section 3) are indicative only of the overall stability (exciting beam + detection electronics) of the experimental system. However, this does not affect the validity of the separation of the time-windowed spectra into fast (picosecond) and slow (nanosecond) classes of components differing in lifetimes by three orders of magnitude.

The pulse-width limitation of the ACO synchrotron compared with sub-picosecond laser excitation is offset by several other advantageous characteristics among which we note the day-long stability of the source and, most important for the present work, the ease and wide-range of tunability in the ultraviolet. We routinely scan excitation wavelengths between 230 and 358 nm in 'up-down-up' sequences of data accumulation, a range of 15 550 cm^{-1} at a rate of 26 cm^{-1}/s, a capability not available in any laser source. This capability, in conjunction with time-windowed detection, has allowed us to obtain time-windowed excitation spectra which complement the more common time-windowed emission spectra. This has extended considerably our ability to interpret the photophysics of these systems.

In this paper we present results of three types of experimental data: (i) Emission decay data at various emission wavelengths. Global analysis of this data on the basis of a two-exponential model gives us effective lifetimes of the picosecond and nanosecond classes of emissions. (ii) Time-windowed emission spectra. Deconvolution of these, using lifetimes obtained in (i), leads to time-resolved emission spectra of the picosecond and nanosecond components. (iii) Time-windowed excitation spectra which, deconvoluted in a similar way, lead to excitation spectra of the same time-resolved species.

For both d(AT) and d(TA) the results from these different experiments find a satisfactory basis for interpretation in the two-state stacked/unstacked model. The picosecond species turn out to have the emission and excitation characteristics of the monomer chromophores A and T, consistent with their origin in the unstacked fraction. The excitation spectra of the nanosecond species, however, are identical with the absorption spectrum of the layered co-crystal of A and T in the direction between and perpendicular to the base planes. The long-lived (nanosecond) emissions must then have their origin in a stacked ground state and hence should be classified as 'excited dimer' rather than as 'excimer' or 'exciplexes.' These results constitute direct experimental evidence that the nanosecond species originate from absorption by the stacked fraction of the systems and provides confirmation, 25 years after the first report [29], that the stacking of the bases leads to significant changes in their energy levels and transitions in addition to the hypochromic changes in intensity.

2. Experimental

A full description of the ACO synchrotron excitation facility at LURE has been given by Guyon et al. [6]. A description of the SLM 2800 spectrofluorimeter and the associated photon-counting electronics at the ultraviolet/visible port has been given in our earlier papers [1,2] while details of the procedures for the collection of time-windowed spectral data and decay profile data for the lifetimes analysis are given in ref. 7. We point out the use of a double monochromator in the excitation beam. Fluorescence intensities showed no evidence of non-linear effects.

Decay data for three emission wavelengths 350, 400 and 460 nm have been fitted to models of two or three independent, exponentially decaying components by reiterative convolution with the instrumental excitation pulse profile. Fitting is by non-linear least-squares minimization using the Marquardt algorithm, the goodness-of-fit criteria being the visual randomness of the time distributions of the weighted residuals and their auto-correlation function, together with the value of χ^2. All data sets for a given system and set of conditions have also been analyzed globally [8,9]. In all cases a wide variety of initial values were used to avoid false minima situations.

All spectra have been corrected for instrumental and beam parameters. Emission spectra have been corrected for the wavelength-dependent response of the emission monochromator and photomultiplier from 300 to 550 nm using factors determined for *p*-terphenyl in ethanol by Privat, Wahl and Brochon (J.-C. Brochon, personal communication) based on the corrected spectrum of Berlman [10]. The correction factors were determined at 5-nm intervals and have been interpolated to 2-nm intervals for use with our data. For excitation spectra corrections have been made for the absorbance of the solutions at 2-nm intervals over the range of exciting wavelengths down to 230 nm using the method of Vigny and Duquesne [11] and the wavelength variation of exciting beam intensity at the position of the sample has been obtained using solid sodium salicylate deposited on a silica plate placed at 45° to both excitation and emission axes.

For a fluorescing system consisting of independent, exponentially decaying emitters with different lifetimes, the impulse response function to a delta excitation pulse can be written as

$$I_f(\lambda,t) = \sum_i \alpha_i(\lambda) \exp - t/\tau_i,$$

showing that the system will exhibit wavelength-dependent decay profiles and time-dependent spectra. For a finite exciting pulse $E(t)$, the actual response function $B(t')$ is then the convolution of the impulse response function with the exciting pulse profile.

$$I_f(\lambda,t') = \sum_i (\alpha_i(\lambda) \cdot B_i(t'))$$

$$= \sum_i \alpha_i(\lambda) \int_0^{t'} E(t') \times \exp - (t' - t)/\tau_i \, dt$$

The observed spectrum at any instant in time is thus a mixture of time-independent constituent spectra $\alpha_i(\lambda)$, each weighted by its convolution

integral $B_i(t')$. In practice the spectra are observed over a finite time interval $t' = u \rightarrow t' = v$, the time window, and so the weighting coefficients $C_i|_u^v$ are integrals of $B_i(t')$ over this range.

$$C_i|_u^v = \int_u^v B_i(t')\,\mathrm{d}t'$$

$$= \int_u^v \left[\int_0^{t'} E(t') \exp -(t'-t)/\tau_i \,\mathrm{d}t \right] \mathrm{d}t'$$

The time-windowed emission spectrum can then be written as

$$I_f(\lambda)|_u^v = \sum_i \alpha_i(\lambda) \cdot C_i|_u^v$$

or more simply as $I_f(\lambda, j) = \Sigma \alpha_i(\lambda) \cdot C_{ji}$ where j indexes the various time windows ($j = 1$ corresponds to $\Delta t' = u \rightarrow v$; $j = 2$ corresponds to $v \rightarrow w$, $j = 3$ to $w \rightarrow x$, etc.) so that C_{ji} constitutes a matrix of weighting coefficients. These coefficients are evaluated for the specific time windows from the decay functions using the lifetimes obtained from the appropriate lifetime analysis. The time-independent emission spectra, $\alpha_i(\lambda)$, are then obtained from the experimental time-windowed spectra $I_f(\lambda, j)$ as

$$\alpha_k(\lambda) = \sum_l D_{kl} \cdot I_l(\lambda)$$

where D_{kl} is the matrix inverse of C_{ji}. As a matter of terminology we note that the $\alpha(\lambda)$ are the 'decay-associated spectra' (DAS) introduced by Knutson et al. [12] and used to describe the behavior of non-interacting individual species in mixtures ('heterogeneity'). When excited-state reactions occur then DAS may still be computed but they no longer represent real emission spectra. For situations such as this, Lofröth [13] has shown how DAS may be converted to 'species-associated spectra' (SAS) if an appropriate and correct model for the excited-state reaction is available.

A more direct way of relating emission spectra to ground states, and thus searching for heterogeneity in unknown situations, is to investigate the excitation spectra which correspond to the time-resolved emission spectra, the so-called 'time-resolved excitation spectra' for which we reported the first examples in adenosine [14] and its derivatives [7]. Time-resolved excitation spectra can be extracted from time-windowed excitation spectra by writing the impulse response function in the expanded form

$$I_f(\lambda_{ex}, \lambda_{em}, t) = \sum_i \sigma_i(\lambda_{ex}) \cdot \alpha_i(\lambda_{em}) \exp - t/\tau_i$$

where σ represents an absorption cross-section and wavelength-independent quantities such as species concentration and quantum yield are neglected. Following the above treatment of exciting pulse convolution and time-window effects then leads to the excitation spectra corresponding to time-resolved emissions.

In the present work the same three time windows have been used for both excitation and emission spectra, viz., 0–2.35, 2.35–4.70 and 4.70–36.0 ns. All computations have been carried out on a VAX 750 or an IBM PC/XT.

d(AT) and d(TA), purity greater than 99% by TLC and HPLC, were obtained from Sigma and were used as supplied. Solutions $A_{260} \leq 1$, corresponding to concentrations of approx. 5×10^{-5} M were prepared in neutral dilute buffer solution (Tris, NaCl) at pH 7.2 and absorption spectra were measured for each solution on a Cary 118 CX spectrophotometer.

3. Results

3.1. Decay kinetics

Time profiles have been fitted over the rising part of the response so well as the decaying part in order to provide extended goodness-of-fit criteria and the data have been analyzed independently at each emission wavelength as well as globally.

As expected, inspection of log plots of the decays shows a single-exponential response function to be inadequate. Consequently, we have analyzed the decay data using a bi-exponential function with the results shown in table 1 and it can be seen that a large fraction of the emission (from 30 to 70%, depending on λ_{em}) decays in the nanosecond time range. The results are reasonably self-consistent, as may be seen by inspecting the percentage emissions obtained by independent and global analyses.

Table 1

Independent and global analysis for impulse response functions

d(TA); λ_{ex} = 260 nm					
λ_{em}(nm)	f_1 [a](%)	τ_1(ns)	f_2[a](%)	τ_n(ns)	χ^2
Model: bi-exponential; independent analysis					
350	70.1	0.055	29.9	5.00	1.80
400	47.0	0.049	53.0	4.20	1.51
460	30.8	0.114	69.2	5.96	1.95
Model: bi-exponential; global analysis					
350	69.3	0.048	30.7	4.66	1.84
400	46.5	0.048	53.5	4.66	
460	27.8	0.048	72.2	4.66	
d(AT); λ_{ex} = 260 nm					
λ_{em}(nm)	f_1(%)	τ_1(ns)	f_2(%)	τ_2(ns)	χ^2
Model: bi-exponential; independent analysis					
350	62.4	0.053	37.6	4.17	1.39
400	39.8	0.103	60.2	3.84	1.99
460	30.2	0.199	69.8	4.82	1.60
Model: bi-exponential; global analysis					
350	63.2	0.054	36.8	3.71	2.10
400	35.5	0.054	64.5	3.71	
460	24.3	0.054	75.7	3.71	

[a] f_i: percent emissions, given by $f_i = (\alpha_i\tau_i/\Sigma_i\alpha_i\tau_i)100$.

The globally obtained lifetimes for the nanosecond emissions of d(TA) and d(AT) are 4.7 and 3.7 ns, respectively, a difference which we believe to be real and which we show later finds an explanation in the spectral studies.

The independent lifetimes show an unwelcome spread around the global values and the χ^2 values for the global analyses are not an improvement on the independent values despite the decrease in number of degrees of freedom. This is most probably due to the weakness of the emissions and the low number of counts which we are able to collect despite the considerable brightness of the ACO source. A measure of the dimness of our system is that the absorbance × quantum yield product $A\phi_f$ is approx. 10^{-4} while for tryptophan it is about 10^{-2}. Consequently, while good lifetime data for tryptophan systems can be collected in a few minutes with flashlamp excitation [12,13] the data presented and analyzed here take approx. 50 min to acquire, not counting background and pre- and post-flash runs. Longer exposures encounter problems of beam decay and increased risk of photochemical degradation. Much higher counts (maxi-

Table 2

Tri-exponential response function analyses

λ_{em}	f_1 [a](%)	τ_1	f_2 [a](%)	τ_2	f_3 [a](%)	τ_3	χ^2
d(TA); λ_{ex} = 260 nm, independent analyses							
350	61.9	0.049	17.8	4.07	13.1	5.88	1.76
400	46.1	0.043	18.3	3.0	35.7	5.7	1.57
460	30.3	0.129	11.4	2.26	58.4	8.7	1.91
d(TA) λ_{ex} 260 nm, global analysis							
350	66.2	0.042	7.9	2.53	26.0	6.27	1.83
400	43.0	0.042	19.3	2.53	37.7	6.27	
460	24.8	0.042	8.9	2.53	66.3	6.27	
d(AT); λ_{ex} 260 nm, independent analyses							
350	55.3	0.036	15.3	1.96	29.5	6.37	1.27
400	18.1	0.077	31.2	1.41	50.8	6.67	1.36
460	24.3	0.116	18.2	1.77	57.5	6.63	1.77
d(AT); λ_{ex} 260 nm, global analysis							
350	59.6	0.049	16.3	2.54	24.1	6.81	1.69
400	32.3	0.049	43.5	2.54	24.2	6.81	
460	21.9	0.049	30.5	2.54	47.7	6.81	

[a] f_i: percent emissions, given by $f_i = (\alpha_i\tau_i/\Sigma_i\alpha_i\tau_i)100$.

mum) are obtained using mode-locked frequency-doubled laser excitation [15,16] at 290 nm, but such arrangements are not capable of continuous wide-ranging excitation-wavelength studies. In the instances in which our results for other systems, e.g., poly[d(GC)], can be compared with laser excitation work, it is gratifying to note that we obtain quite similar values of the parameters [32], indicating that our use of lower cumulative data counts does not lead to serious inaccuracies.

In view of the results obtained for the time-resolved emission spectra (vide infra) it became of interest to see how the decay results would respond to analysis on the basis of a tri-exponential response function. The results of such analyses are given in table 2. In general, the effect is to split the nanosecond lifetime into two components, leaving the picosecond component unchanged from the bi-exponential analysis. Consistency between the independent and global analysis is somewhat worse than for the bi-exponential model and the χ^2 values are only marginally better, though this might be anticipated from the increased number of fitting parameters. The significant result from these analyses is that the global nanosecond lifetimes for the sequence isomers are very similar, at 2.53 and 6.27 ns for d(TA) and 2.54 and 6.81 ns for d(AT). The coincidence of the shorter lifetimes is obviously fortuitous but it is not unreasonable to suggest that the longer lifetimes are identical within $\pm 10\%$. Standing alone, the results of the tri-exponential lifetime analyses could not be considered unequivocal evidence for a three-component model of these systems. But it will be seen that they are consistent with and support the results from time-resolved spectra.

3.2. Time-resolved emission spectra

Based on the minimal two-component global kinetic description of these systems, the deconvolution of the observed time-windowed spectra into time-resolved spectra gives the results shown in figs 1 and 2 (all deconvoluted spectra are presented unsmoothed). The picosecond component spectra for d(AT) and d(TA) are essentially identical, having $\lambda_{max} \sim 320$ nm and $1/2\lambda_{max} \sim 345$ nm.

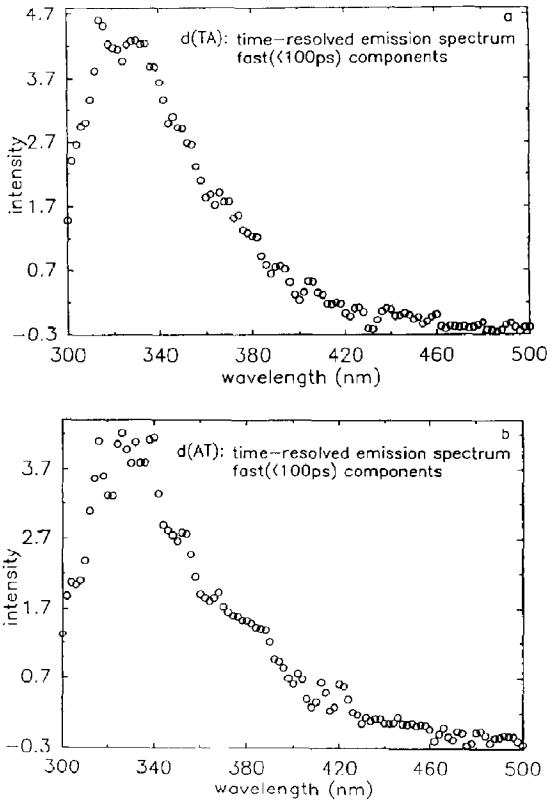

Fig. 1. Time-resolved emission spectra for components with lifetimes less than 100 ps; $\lambda_{ex} = 260$ nm. (a) d(TA), (b) d(AT).

By contrast, the nanosecond spectra differ both from the picosecond spectra and from one another. The nanosecond spectra, as well as being red-shifted from the picosecond spectra, are much broader ($\Delta\bar{\nu}_{1/2} \sim 10\,800$ cm^{-1} vs ~ 4500 cm^{-1} for the picosecond spectra). Despite the noise there is indication of some structure. Accordingly they have been fitted by an unrestricted least-squares Gaussian program, with the results shown in fig. 3a and b, the relevant parameters being given in table 3.

Relative to the areas of the Gaussians the low value of the residuals is noteworthy, indicating that the noise is almost entirely random. The resolution of each spectrum into two Gaussians seems to constitute a good description of the data. Although no attempt has been made to force a fit

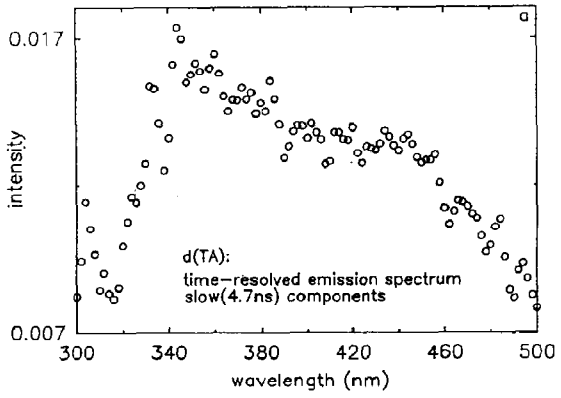

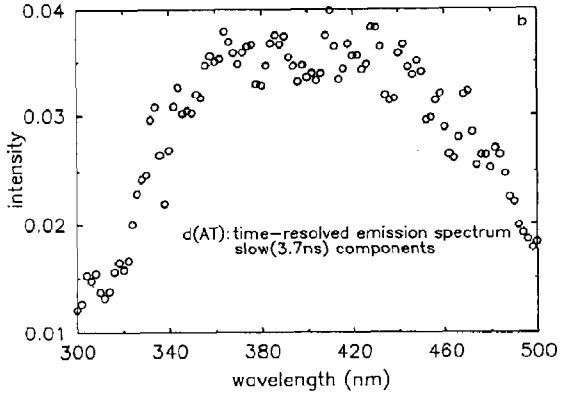

Fig. 2. Time-resolved emission spectra for components with lifetimes in the nanosecond range. Optical parameters same as in fig. 1. (a) d(TA), (b) d(AT).

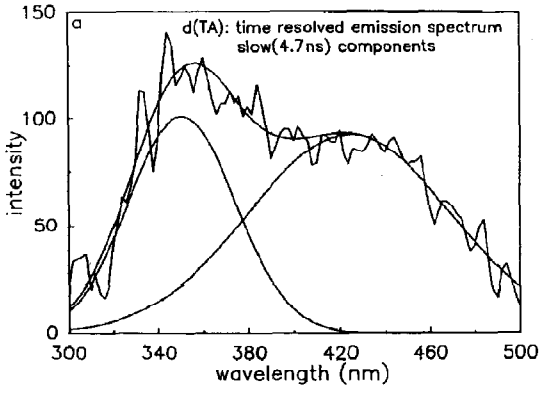

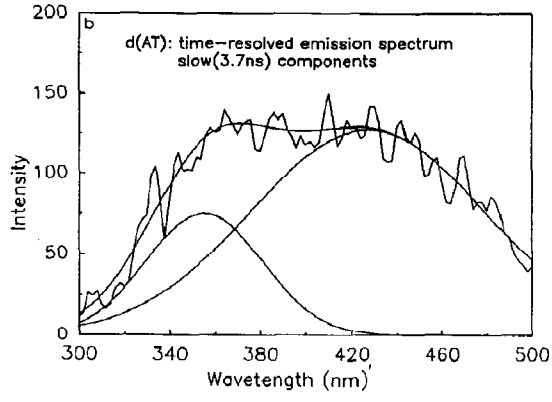

Fig. 3. Gaussian fits to fig. 2; the experimental points have been connected; numerical parameters are given in table 3. (a) d(TA), (b) d(AT).

to the same Gaussians for both d(TA) and d(AT), the component Gaussians are very similar in position and width in d(AT) and d(TA), differing mainly in their relative intensities. Normalizing the spectra so that the integrated intensity of lower energy component I is the same in d(AT) and d(TA), then component II is twice as intense in d(TA) as in d(AT).

3.3. Time-resolved excitation spectra

The spectra of the picosecond components of d(AT) and d(TA) are quite similar to each other

Table 3

Parameters of Gaussian [a] fitting to the nanosecond lifetime time-resolved spectra of d(TA) and d(AT)

	Gaussian I			Gaussian II			
	λ_0 (nm)	σ (nm)	No.	λ_0 (nm)	σ (nm)	No.	Σ residuals
d(TA)	425	63	10171	351	33	5967	100
d(AT)	428	72	16291	355	36	4841	104

[a] Gaussians are taken in the form $I(\lambda) = \text{No.}/\sigma\sqrt{\pi}\ \exp-((\lambda-\lambda_0)/\sigma)^2$.

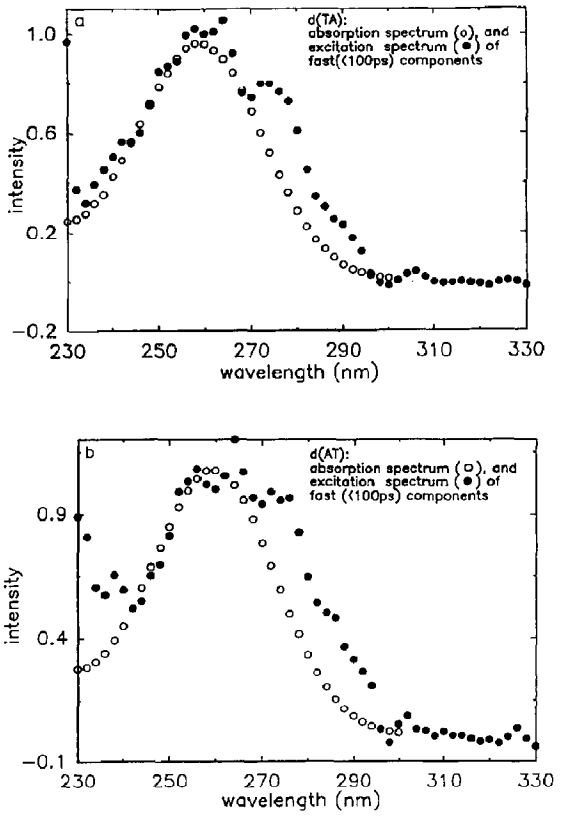

Fig. 4. Time-resolved excitation spectra of the fast ($\tau < 100$ ps) components. Comparison is made with the solution absorption spectrum in each case. (a) d(TA), (b) d(AT).

and to the solution absorption spectra (fig. 4a and b). The major difference between the two excitation spectra lies below 245 nm where the d(TA) spectrum fits the absorption quite closely while the d(AT) spectrum shows a marked divergence. Both excitation spectra are broadened relative to their absorption spectrum on the low-energy side.

The nanosecond excitation spectra of d(TA) and d(AT) are essentially superimposable (fig. 5a and b). They bear no obvious relationship to the isotropic solution absorption spectra and present a most unusual aspect, having an almost linear increase with decreasing wavelength from an onset of approx. 310 nm. An assignment of these spectra is presented below.

Discussion

4.1. Correlation of emitting states and fluorescence lifetimes

In section 3 we have presented evidence that time-resolved emission and excitation spectra can be separated into two classes having lifetimes differing by three orders of magnitude. This separation is internally consistent in that the resolved picosecond emission spectra of d(AT) and d(TA) are identical (fig. 1) as are the corresponding excitation spectra (fig. 3). This is in accord with expectations based on the two-state stacked/unstacked model in which the picosecond emis-

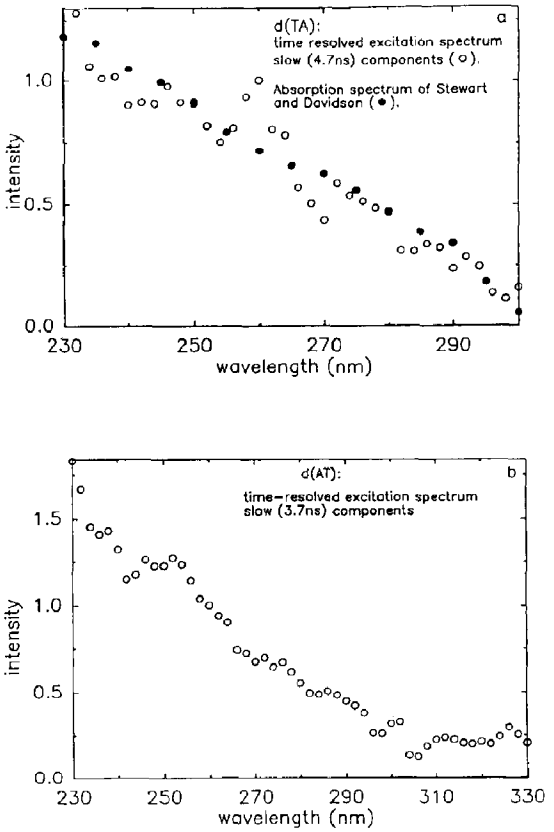

Fig. 5. Time-resolved excitation spectra of the nanosecond emission spectra. Comparison is made with the anisotropic absorption spectrum of co-crystals of 9-MeA and 1-MeT (Stewart and Davidson [29]; loc. cit.). The fit shown has not been optimized. (a) d(TA), (b) d(AT).

sion originates from the unstacked fraction which consists of A and T in equimolar proportions in both d(AT) and d(TA). This model also suggests that the picosecond spectra consist of two very fast components. Although resolution of these spectra into separate A and T components is obviously beyond the capability of our instrumentation, these systems provide an interesting challenge for those with low picosecond instrumentation.

There is also clear evidence that the nanosecond class of emissions contains two components (fig. 2 and table 3), and the question arises as to whether these represent two independent states with different lifetimes or whether the two states decay with the same lifetime, characteristic of a common precursor. To investigate this was the motivation for carrying out the tri-exponential response analyses reported in table 2. The significant results from these are that d(TA) and d(AT) have essentially identical τ_2 values (2.53 and 2.54 ns) and τ_3 values (6.27 and 6.81 ns). This lends support to the idea, arising from the Gaussian analysis of the nanosecond emission spectra, that d(TA) and d(AT) have the same or very similar excited states which are produced in different proportions. This model implies that the τ_2 obtained from the bi-exponential analysis are the weighted means of the true lifetimes. If the bi-exponential lifetimes are reasonably precise (so that the difference between 4.7 and 3.7 ns is significant) and if the Gaussian resolutions of fig. 2 and table 3 are correct, then the weighted bi-exponential nanosecond lifetimes of d(TA) and d(AT) can be resolved into lifetimes of states I and II (the nanosecond component states, numbered in order of increasing energy). The results of this, that $\tau(\mathrm{I}) = 2.3$ ns and $\tau(\mathrm{II}) = 6.1$ ns, are in substantial agreement with the global tri-exponential lifetimes analyses, and we conclude that lifetime and spectral results are both consistent with the idea that the same two independently emitting nanosecond-lifetime states result from the excitation of d(TA) and d(AT).

Few other lifetime and spectral studies relevant to our systems have been published. Using a synchronously pumped ring dye laser with intracavity frequency doubling to 290 nm, Kobayashi et al. [15a] have obtained an exciting pulse width of 5 ps and have used this with a polychromator streak camera/multi-channel plate detector into an SIT/OMA to determine the single-exponential fluorescence lifetime of 9-methyladenine as 5 ps [15b]. This is compatible with the assumptions of this paper and their emission spectrum is similar to our fig. 1. Exciting similarly at 290 nm with a 6 ps pulse and a 43 ps response function, Rigler et al. [16a] have observed bi-exponential decays of ATP with lifetimes of 290 ps and 4.17 ns, together with an apparently single-component emission spectrum with $\lambda_{max} \sim 400$ nm. Poly d(AT) showed a bimodal total emission spectrum with $\lambda_{max} \sim 330$ and 410 nm and the decays were variously analyzed as bi-exponential ($\tau_1 = 94$ ps, $\tau_2 = 870$ ps, $\chi^2 = 2.1$) [16b] or tri-exponential (90 ps, 870 ps and 8.64 ns, $\chi^2 = 2.0$). No assignment of spectra or correlation with lifetimes has been given. Both ATP and poly [d(AT)] thus show complexities not anticipated from the behavior of 9-methyladenine and the d(TA)/d(AT) results presented here.

4.2. Excitation spectra for nanosecond emissions

We have found that the excitation spectrum for the transition which excites the nanosecond emission coincides with the anisotropic absorption perpendicular to the molecular planes in the crystal of the 1 : 1 hydrogen-bonded complex of 1-methylthymine with 9-methyladenine [29]. This spectrum is obviously incomplete, showing a continually rising absorption from an onset around 300 nm to the limit of observation at 230 nm (fig. 4). However, it is sufficient to demonstrate the absence of any characteristics attributable to exciton splitting. Stewart and Davidson [29] suggest this perpendicular absorption may be due to normal $n \rightarrow \pi^*$ transitions in the adenyl group but it is not obvious that this will account for the considerable width of the transition (at least 8000 cm^{-1}) or its intensity (oscillator strength at least 2×10^{-2}).

The crystal structure shows extensive vertical stacking of T on T and A on A. For T stacking, the $C_4 = O$ carbonyl group of one T is directly centered over the adjacent T, and for A stacking the $N_3 = C_2$ group overlaps directly the pyrimidine ring of an adjacent A. It is possible that

vertical interactions rather than $n \rightarrow \pi^*$ transitions may be responsible for the observed absorption. Further work, both experimental and theoretical, is needed to elucidate the nature of this transition, but regardless of this uncertainty the correlation shown in fig. 5 is strong evidence that the nanosecond emissions in solution are due to the excitation of vertically stacked bases.

4.3. Assignment of nanosecond emitting states and correlation with structures

The origin of the nanosecond emissions as resulting from the excitation of stacked bases clearly supports their assignment as excimer-like, or more correctly excited-dimer emissions. That is, a true excimer would have the same excitation spectrum as the monomer whereas our emissions have the same excitation spectra as the stacked bases. The transition to stacked ground state then directs attention to the relation of the d(TA) and d(AT) nanosecond emission spectra to the extent of stacking and stacking geometry in these isomers.

Information on the ground-state structures of d(TA) and d(AT) is sparse. A crystal structure (non-single crystal) has been reported for the Et_4N^+ salt of T_pdA [17] in which one TA is related to the next by a left-handed screw translation and Hoogsteen hydrogen-bonding is invoked. There is AA overlap, but no TT or AT overlap and in this respect the structure may be compared to that of the A/T co-crystals reported by Stewart and Davidson [29] which has AA and TT overlap but no AT overlap. No crystal structure has been reported for d(AT). Single-crystal studies [18] on the tetranucleotide d(pApTpApT) show a classical Watson-Crick geometry in which 'T is tightly stacked on A but there is no stacking of A on T within one molecule' and the repeat unit is a dinucleotide, the 'alternating-B' structure. Fiber X-ray studies on poly[d(AT)] show it can adopt a variety of forms [19] depending on the degree of hydration, method of preparation, nature and concentration of excess salt, etc. Models to interpret these data usually assume a right-handed helix with Watson-Crick base pairing but Hoogsteen pairing in a left-handed helix has been proposed by Drew and Dickerson [20] while Gupta et al. [21] suggest a left-handed helix with Watson-Crick pairing.

For solutions, sequence effects have been reported for NMR studies of d(TA) and d(AT) but the shifts do not correspond to B, A or A′ geometries or a mixture of them [22]. More results are available for poly[d(AT)]. 2D-NMR and NOE studies [23] are mostly consistent with a 'B' structure but there is evidence for a dispersion of chemical shifts, implying that slightly different conformations can exist within the poly[d(AT)] helix. Linewidths are larger than expected from T_2 measurements, suggesting that these discrete conformational states are slowly interconverting. Evidence from ^{31}P-NMR shows two resolved signals of equal area, indicating the existence of two distinct alternating phosphodiester conformations [24], behavior which is more pronounced in the presence of 1 M Me_4N^+ [25].

In general, there is evidence for the existence (and perhaps co-existence) of a variety of conformations of A/T oligomers, both in solid and in solution phase, leading to a different overlap of the stacked bases. However, an extensive, detailed description of the conformations, with particular attention to base-overlap geometry and population distribution, is not available for dilute aqueous solutions of d(TA) and d(AT). Consequently, no direct correlation can presently be made between known conformations and emitting states. However, the problem may be approached indirectly by analogy with other systems.

The spectral behavior which we report here has been observed earlier in polarization-resolved spectroscopy of CpA [5a] and ApC [5b] which also produced two classes of spectra associated with the stacked fractions of each isomer, a broad one at λ_{max} 435 nm with $\sigma = 50$ nm and a narrower one at $\lambda_{max} \sim 365$ nm with $\sigma \sim 35$ nm. The similarity of the position and width parameters to those of d(AT) and d(TA) in table 3 is striking and suggests we may be observing luminescence consequences of the same sort of stacking behavior. The stereochemistry of stacked (closed conformer) forms of DNPs has been discussed thoroughly by Lysov et al. [26] who have taken into the account the four possible combinations of face/back orientations for the two nucleic acid

bases in both right-handed and left-handed helical geometry, giving eight types of base-stacking geometries. By self-consistently fitting ultraviolet, CD and NMR data, computing the energies of conformers by the method of atom-atom potentials [19] and transforming these results to a room-temperature aqueous solution situation, they have established the most likely major stacked conformers, their geometries and population distribution at room temperature for ApA, ApC, CpA and CpC [20]. Using this information, the luminescence results for the AC/CA systems could be accounted for if the low-energy transition I results from excitation of a left-handed conformation, probably M^{bb}, while the higher energy transition II results from excitation of the predominant right-handed conformation P^{ba} [5a,b]. The work of this group has not extended to the deoxy-DNPs and so quantitative correlation with our results cannot be carried out. Nevertheless, the qualitative correlation between the r(A,C) and the d(A,T) systems is so obvious that we feel justified in proposing that the same conformational origins may be in effect. This is in line with recent theoretical work [30] indicating that the alternating double-helical poly[d(AT)] should be capable of existing in the left-handed Z-form and we note that left-handed stacking of the AT pair has been observed [31] in the crystal structure of $d(m^5CGTAm^5CG)$. Furthermore, a pronounced dominance of a broad emission at $\lambda > 400$ nm, similar to emission I of d(TA) and d(AT), has been observed for a Z-form oligomer, duplex $d(CG)_3$, both in saturated solution and in crystalline form [32].

Comparison of the excitation and emission spectra of the nanosecond species is of interest in two respects. First, the pronounced lack of symmetry between excitation and emission implies a considerable structural relaxation in the excited state. Second, it draws attention to the spectroscopic origin of the two relaxed states. Are they both produced from the same initially formed Frank-Condon state, or does the act of absorption produce two FC states which individually relax to emitting states? The present work provides no evidence allowing us to distinguish between these probabilities as the excitation spectra (fig. 5a and b) are only quantitatively different. These considerations apply equally to both d(TA) and d(AT), the situation being represented in fig. 6.

The differing relative intensities of I/II in d(TA) and d(AT) could be simply accounted for on the basis of differential population of these FC excited states from different stacking geometries in the ground state. In the B or alternating-B structures of DNA, sequence isomers such as d(TA) and d(AT) exhibit quite different overlaps of the chromophores [18,19], and it is not unreasonable that such structures may have different

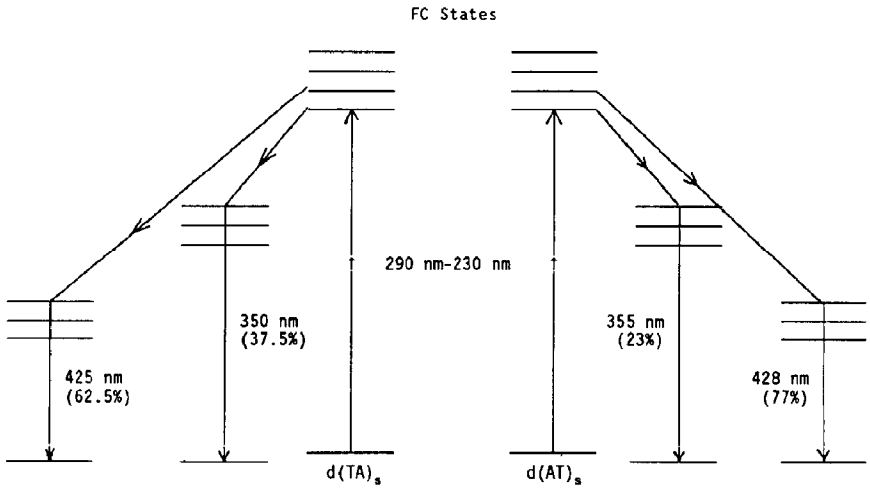

Fig. 6. Excited-state pathways for nanosecond states of stacked d(TA) and d(AT).

emission spectra. However, the occurrence of two emission spectra for each of the isomers requires that each isomer exists in two stacked conformations, and as suggested above those may be the right-handed B or alt-B and the left-handed Z structures.

4.4. Implication for energy transfer and photochemistry

The possibility of energy transfer between the major bases of DNA has often been discussed but little experimental evidence is available. The results which we report here are relevant to several aspects of energy transfer, namely, energy transfer between unstacked bases, energy transfer from unstacked bases to stacked bases, and energy transfer between stacked bases.

The fast (< 100 ps) time-resolved emission spectra for d(TA) and d(AT), which we attribute to emission from the unstacked bases, have indications of individual T and A emissions, particularly in the d(TA) spectrum which is less noisy at the maximum than the d(AT). If no energy transfer occurs, then from the fractional absorptions of T and A together with the quantum yields of fluorescence, the spectrum (fig. 1) should be composed of approximately equal proportions of T and A fluorescence. Although this may be the case, the resolution of this curve is not unambiguous; empirically, it may also be construed to be mostly T with a little A, or vice versa. So we can only conclude that we have no evidence requiring the occurrence of energy transfer between monomers, but should it occur it can only be partial. Absence of energy transfer between unstacked monomers would not be surprising in view of dipole orientation effects, distance dependence and the lack of overlap between emission and absorption spectra.

Concerning the stacked states, energy transfer to them from the unstacked monomers can be ruled out by the observed excitation spectra (fig. 5) for if energy transfer were to occur the excitation spectra would be the same as the normal (isotropic) monomer absorption for 100% transfer and would have a weighted monomer contribution for less than 100% transfer. In no way can the observed spectrum be construed to contain any monomer absorption. Energy transfer between the stacked dimer states is ruled out by their independent first-order decays.

The photophysics which we have investigated here can be related to photochemical changes in d(TA) and d(AT). Photolysis of d(TA) at 254 nm leads to the formation of a cyclobutane-type photoadduct between T and A, with bonding between the $C_5 = C_6$ of T and the $C_5 = C_6$ of A [33]. The reaction seems to occur at the singlet level as it is not sensitized by acetone (a triplet sensitizer) and would seem to require a very specific geometry of the chromophores. Of particular interest is the fact that the reaction is sequence-specific and does not occur (or occurs much less efficiently) with d(AT). If one of the excited states studied here is a precursor to this photo-product, the sequence specificity would suggest that it relates to state II ($\lambda_{max} \sim 350$ nm) as this is relatively twice as abundant in d(TA) as in d(AT). Furthermore, although the overall photochemical quantum yield in d(TA) is approx. 7×10^{-4} [33a] referred to total photon absorption, if only the specific absorption between the chromophore planes is responsible (as in our excitation spectra) then the photochemical quantum efficiency of these photons is much higher (roughly by the ratio of the in-plane and perpendicular absorption coefficients) at approx. 0.15. These considerations indicate a potentially greater importance for this type of photo-adduct formation in photobiology than has previously been assumed.

Acknowledgements

We thank Dr J.-C. Brochon for facilitating our access to the ultraviolet-visible fluorescence facility at LURE in the limited time available and for the emission spectrum correction data. Ding-guo Hu (Beijing University and OSU) implemented the global analysis program for the fluorescence decay data and wrote the programs for the deconvolution of the time-windowed emission and excitation spectra. Data treatment was carried out by Yin-jian Fu, and Dr L.P. Hart helped in many ways. This work would not have been possible without the support of PHS Grant 30474.

References

1 J.-P. Ballini, M. Daniels and P. Vigny, Biophys. Chem. 18 (1983) 61.

2 J.-P. Ballini, M. Daniels and P. Vigny, J. Luminescence 27 (1982) 389.

3 a J.P. Morgan and M. Daniels, Photochem. Photobiol. 27 (1978) 73.
b J.P. Morgan and M. Daniels. Chem. Phys. Lett. 67 (1979) 533.

4 a M. Daniels and J.P. Morgan, Chem. Phys. Lett. 58 (1978) 283.
b J.P. Morgan and M. Daniels, Photochem. Photobiol. 31 (1980) 101, 207.

5 a C.S. Shaar, J.P. Morgan and M. Daniels, Photochem. Photobiol. 39 (1984) 747.
b M. Daniels, C.S. Shaar and J.P. Morgan, Biophys. Chem. 32 (1988) 229.

6 P.M. Guyon, C. Depautex and G. Morel, Rev. Sci. Instrum. 47 (1976) 1347.

7 J.-P. Ballini, M. Daniels and P. Vigny, Eur. Biophys. J. 16 (1988) 131.

8 J.R. Knutson, J.M. Beecham and L. Brand, Chem. Phys. Lett. 102 (1983) 501.

9 S.L. Frye, K. Jaeju and A.M. Halpern, Photochem. Photobiol. 40 (1984) 555.

10 I. Berlman, Handbook of fluorescence spectra of aromatic molecules (Academic Press, New York, 1985).

11 P. Vigny and M. Duquesne, Photochem. Photobiol. 20 (1974) 15.

12 J.R. Knutson, D.G. Walbridge and L. Brand, Biochemistry 21 (1982) 463.

13 J.-E. Lofröth, J. Phys. Chem. 90 (1986) 1160.

14 J.-P. Ballini, M. Daniels and P. Vigny, in: Light in biology and medicine, eds R.H. Douglas, J. Moan and F. Dall'Acqua (Plenum, New York, 1988) p. 31.

15 a S. Kobayashi, M. Yamashita, T. Sato and S. Muramatsu, IE^3, J. Quant. Elect. QE-20 (1984) 1383.
b M. Yamashita, S. Kobayashi, K. Torizuka and T. Sato, Chem. Phys. Lett. 137 (1987) 578.

16 a R. Rigler, F. Claessens and O. Kristensen, Anal. Instrum. 14 (1985) 525.
b R. Rigler, F. Claessens and G. Lomakka, Tech. Digest Ultrafast Phenomena, Opt. Soc. Am., Monterey, CA, June 1984, Th. C3-4.

17 H.R. Wilson and J. Al-Mukhtar, Nature 263 (1976) 171.

18 a M.A. Viswamitra, O. Kennard, P.G. Jones, G.M. Sheldrick, S. Salisbury, L. Falvella and Z. Shakked, Nature 273 (1978) 687.
b A. Klug, A. Jack, M.A. Viswamitra, O. Kennard, Z. Shakked and T.A. Steitz, J. Mol. Biol. 131 (1979) 689.
c M.A. Viswamitra, Z. Shakked, P.G. Jones, G.M. Sheldrick, S. Salisbury and O. Kennard. Biopolymers 21 (1982) 513.

19 a S. Arnott and D.W.L. Huckins, Biochem. Biophys. Res. Commun. 47 (1972) 1504.
b S. Arnott and E. Selsing, J. Mol. Biol. 88 (1974) 509.
c S. Arnott, R. Chandrasekaran, D.W.L. Hukins, P.J.C. Smith and L. Watts, J. Mol. Biol. 88 (1974) 523.

20 H.R. Drew and R.E. Dickerson, EMBO J. 6 (1982) 663.

21 G. Gupta, M.H. Sarma, M.M. Dhingra, R.H. Sarma, M. Rajagopalan and V. Sasisekharan, J. Biomol. Struct. Dyn. 1 (1983) 395.

22 R.V. Hosur, G. Govil, M.V. Hosur and M.A. Viswamitra, J. Mol. Struct. 72 (1981) 261.

23 N. Assa-Munt and D.R. Kearns, Biochemistry 23 (1984) 791.

24 a H. Shindo, R.T. Simpson and J.S. Cohen, J. Biol. Chem. 254 (1979) 8125.
b J.S. Cohen, J.B. Wooten and C.L. Chatterjee, Biochemistry 20 (1979) 8125.
c H. Shindo, Eur. J. Biochem. 120 (1981) 375.

25 L.A. Marky, D. Patel and K.J. Breslauer, Biochemistry 20 (1981) 1427.

26 Yu.P. Lysov, V.B. Zhurkin, L.Yu. Tychinskaya and V.L. Florent'ev, Mol. Biol. 13 (1979), 897.

27 V.B. Zhurkin, V.I. Poltev and V.L. Florent'ev, Mol. Biol. 14 (1980), 882.

28 I.D. Bobruskin, B.P. Gottikk, A.M. Dritsyn, Yu.P. Lysov, M.U. Pokrovskaya, L.Yu. Tychinskaya and V.L. Florent'ev, Biophysics 25 (1980) 761.

29 R.F. Stewart and N. Davidson, J. Chem. Phys. 39 (1963) 255.

30 P. DeSantis, S. Morosetti, A. Palleschi and M. Savino, in: Structure and dynamics of nucleic acids, proteins and membranes, eds E. Clementi and S. Chin (Plenum, New York, 1986) p. 31.

31 A.H.J. Wang, T. Hakoshima, G. van der Marel, J.H. Van Boom and A. Rich, Cell 37 (1984) 321.

32 M. Daniels, L.P. Hart, P.S. Ho, J.-P. Ballini and P. Vigny, SPIE 1204 (1990) in the press.

33 a S.N. Bose, R.J.H. Davies, S.K. Sethi and J.A. McClosky, Science 220 (1983) 723.
b S.N. Bose and R.J.H. Davies, Nucleic Acids Res. 12 (1984) 7903.